Available online at www.sciencedirect.com

ScienceDirect

Mendeleev Commun., 2022, **32**, 655–657

Mendeleev Communications

Addition of SiO_2 to the operation of a polyimide cathode in a sodium battery

Alena V. Yudina,[a] Guzaliya R. Baymuratova,[a] Alexander V. Mumyatov,[a] Galiya Z. Tulibaeva,[a] Evgeny N. Kabachkov,[a,b] Pavel A. Troshin,[a] Alexander F. Shestakov[a,c] and Olga V. Yarmolenko*[a]

[a] *Institute of Problems of Chemical Physics, Russian Academy of Sciences, 142432 Chernogolovka, Moscow Region, Russian Federation. E-mail: oyarm@icp.ac.ru*

[b] *Scientific Center in Chernogolovka, Russian Academy of Sciences, 142432, Chernogolovka, Moscow Region, Russian Federation*

[c] *Department of Fundamental Physical and Chemical Engineering, M. V. Lomonosov Moscow State University, 119991 Moscow, Russian Federation*

DOI: 10.1016/j.mencom.2022.09.029

The effect of the addition of SiO_2 nanoparticles on the properties of a polyimide cathode was explored by CV, XPS, and galvanostatic cycling methods. The capacity and average cycling potential of the cell increased in the presence of SiO_2. By quantum chemical modeling, it was shown that SiO_2 nanoparticles served as a framework for polyimide, which retained its fixed structure upon metalation with sodium.

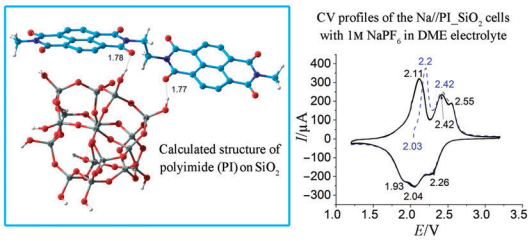

Keywords: polyimide cathode, sodium battery, SiO_2, discharge capacity, quantum-chemical modeling.

The development of sodium-ion batteries (SIBs)[1,2] to replace lithium-ion batteries (LIBs) is of considerable current interest due to the lower cost of Na. The creation of both inorganic and organic electrodes for SIBs has been described.[3–6] An obvious advantage of organic electrode materials is their ability to exhibit redox activity towards Li^+, Na^+, and K^+ ions.

Polymers based on tetracarboxylic acid naphthalene diimide are common cathode materials.[7–10] Polyimide (PI) with bridging CH_2CH_2 groups reversibly undergoes a two-electron redox process (Scheme 1), which corresponds to a theoretical specific capacitance of 183 mAh g^{-1}.

This polyimide was studied as a cathode for LIBs and NIBs,[7–10] and its redox characteristics were reported.[8–9,13] Previously, we found that the LIB PI cathode degraded due to irreversible conformational changes in the polymer chain during lithiation. Therefore, we assumed that the interaction of PI with suitable nanoparticles will contribute to the preservation of its spatial structure during redox processes.

In this work, we studied a nanocomposite electrode based on PI and SiO_2 nanoparticles, which have good adhesion to polyimides used as separators for LIBs.[14–16] Furthermore, SiO_2 is highly compatible with lithium and sodium.[17,18] Addition of SiO_2 reduces dendrite formation on the alkali metal surface during cycling. Aerosil 380 SiO_2 (S = 380 m^2 g^{-1}) with an average particle size of 7 nm was used.

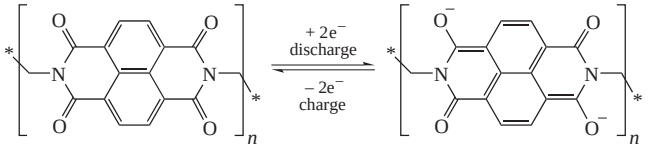

Scheme 1 Polyimide PI redox process.

It was found previously[19,20] that the introduction of Aerosil 380 nanoparticles into a polymer electrolyte increased not only its mechanical strength but also its ionic conductivity. These results suggest that SiO_2 nanoparticles have a positive effect on ion transport in the bulk of the polyimide electrode.

The PI cathode compositions are given in Table 1. The manufacture of cathodes, lithium cells and their study by various experimental methods are described by the well-known procedures.[†]

Table 1 PI cathode compositions (wt%).

Cathode	PI	Carbon black	PVDF	SiO_2
PI cathode	45	45	10	–
PI_SiO_2 cathode	45	45	5	5

[†] A described process,[8] was used to synthesize the polyimide. A published procedure[10] for preparing a nanocomposite PI_SiO_2 cathode was modified at the stage of preparing a solution of the polyvinylidene fluoride (PVDF) polymer binder in *N*-methylpyrrolidone, when the addition of SiO_2 was introduced. Timcal 60 carbon black was used as a conductive additive. The cathode was formed on an Al substrate using DoctorBlade. The weight of the active substance of the polyimide was 0.927 or 0.878 mg in the PI and PI_SiO_2 cathodes, respectively.

Na//PI and Na//PI_SiO_2 cells were assembled with 1 M $NaPF_6$ electrolyte in dimethoxyethane (DME). The CR2032 elements were assembled in an MBraun argon glove box (Germany) using two layers of a Celgard polypropylene separator. Cyclic voltammograms were recorded with a P-2X Potentiostat (Elins, Russia) at a sweep rate of 1 mV s^{-1}.

Cells were tested in the galvanostatic mode on a BTS 5V10mA device from Shenzhen Neware Electronic (China) at a rate of C/5 (73 mA g^{-1}) in a voltage range of 1.5–3.5 V. The 1C current was 365 mA g^{-1}.

The XPS spectra were obtained using a Specs PHOIBOS 150 MCD9 electron spectrometer and an X-ray tube with a magnesium anode ($h\nu$ = 1253.6 eV).[21,22]

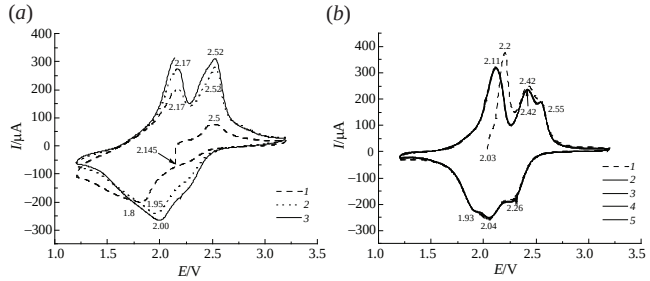

Figure 1 CV profiles of (*a*) the Na//PI and (*b*) Na//PI_SiO_2 cells with 1 M $NaPF_6$ in DME electrolyte. Voltage range, 1.2–3.2 V. Rate, 1 mV s^{-1}.

As shown in cyclic voltammograms (Figure 1), the two-electron metalation process of polyimide has a peak, and the reverse process has two allowed peaks in 1 M $NaPF_6$/DME electrolyte, which indicates an easier flow of the reverse process. In addition, peaks on the cathode and anode branches were more pronounced in the presence of SiO_2 nanoparticles.

An analysis of the XPS spectra showed the presence of a specific interaction between PI and SiO_2 due to the O1s line broadening of SiO_2 [Figure 3(*a*)] and a shift of the Si2p peak [Figure 3(*b*)]. Peaks in the XPS spectra of C1s and N1s remained the same.

Figure 3 shows charge–discharge profiles of Na//PI and Na//PI_SiO_2 cells with 1 M $NaPF_6$/DME electrolyte. The discharge capacity of the Na//PI_SiO_2 cell has a higher capacity compared to the Na//PI cell [Figure 4(*a*)]. The discharge capacities of the PI cathode and PI_SiO_2 cathode were 93 and 110 mAh g^{-1}, respectively, after 300 cycles.

The average voltages of different cells during cycling [Figure 4(*b*)] coincided at the initial stage. However, after the 25th cycle, the average voltage of the PI_SiO_2 cathode began to increase and became 60 mV higher than that for the PI cathode.

For the quantum-chemical modeling of the sodium metalation of a polyimide structure consisting of 2 and 4 units, we used the nonempirical exchange-correlation functional PBE (Perdew–Burke–Ernzerhof)[23] with the pseudopotential SBK (Stevens–Bash–Krauss)[24] and extended basis set C, N, O: [5s, 5p, 2d/3s, 3p, 2d], Na: [4s, 1p/2s, 1p], H: [5s, 1p/3s, 1p] for valence shells. All computations were carried out with the use of the PRIRODA software[25] and computation facilities of the Joint Supercomputer Center of the RAS (Moscow).

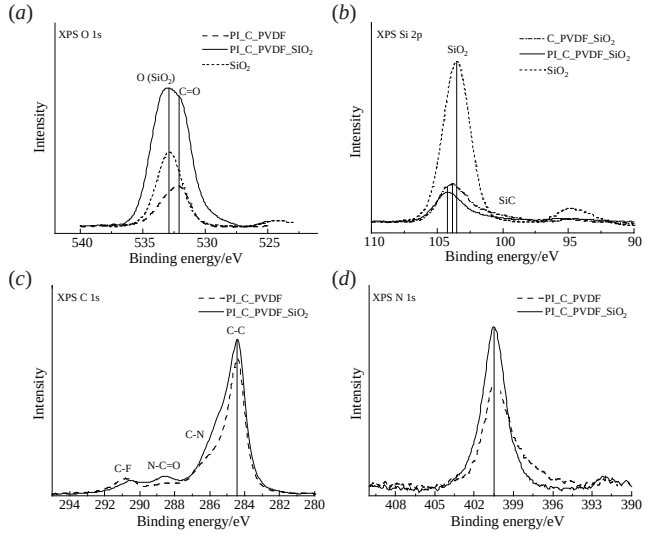

Figure 2 The (*a*) O 1s, (*b*) Si 2p, (*c*) C 1s, and (*d*) N 1s XPS spectra of the polyimide cathode, PI_SiO_2 composite, and SiO_2.

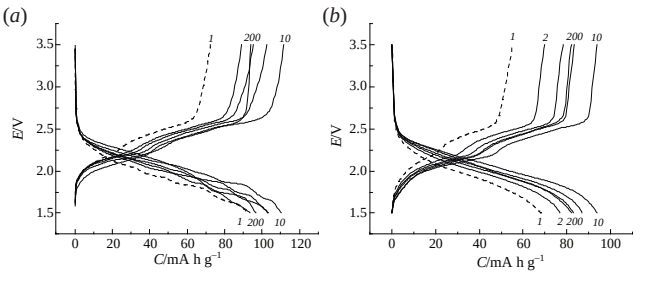

Figure 3 Charge–discharge profiles of (*a*) Na//PI_SiO_2 and (*b*) Na//PI cells. 1 M $NaPF_6$/DME electrolyte. Voltage range, 1.5–3.5 V.

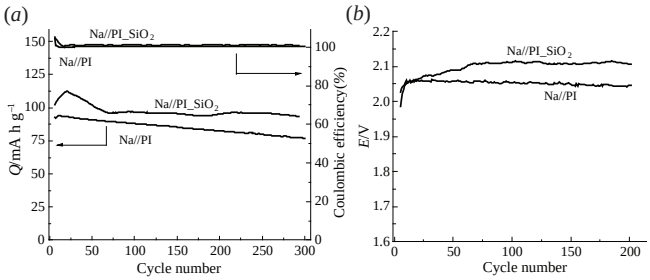

Figure 4 Dependence of (*a*) the discharge capacity and Coulombic efficiency and (*b*) the average voltage *vs*. Na^+/Na on the charge–discharge cycle number for Na//PI and Na//PI_SiO_2 cells.

The PI_SiO_2 nanocomposite was modeled by a hydrated $(SiO_2)_{17}$ cluster of the composition $Si_{17}O_{28}(OH)_{12}$ with an adsorbed polyimide oligomer PI_2 containing two units. Six structures that differed in the coordination and orientation of the polyimide units were found and optimized. The lowest energy structure [Figure 5(*a*)] contained the *trans* conformation of polyimide units; the corresponding structure for the free PI oligomer was higher in energy by 2.50 kcal mol^{-1} than the main *gauche* conformation. The *trans* conformation is appropriate for the formation of two hydrogen bonds C=O···H–O with a total energy of 15.1 kcal mol^{-1}, which is the reason for its stabilization.

The *trans* conformation in the lowest energy structure is retained upon addition of two Na atoms [Figure 5(*b*)]. In this case, the metalation energy of the PI_SiO_2 cluster is 8.3 kcal mol^{-1}

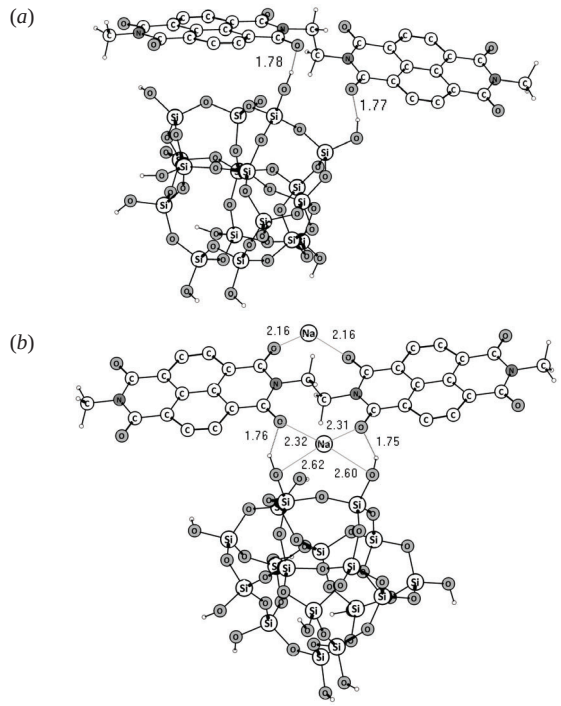

Figure 5 Calculated structures of complexes (*a*) $PI_2Si_{17}O_{28}(OH)_{12}$ and (*b*) $PI_2Na_2Si_{17}O_{28}(OH)_{12}$.

(or 0.18 eV per Na atom) higher than that of the free PI oligomer in the *trans* form. This fact indicates the possibility of a higher energy storage in the case of a nanocomposite electrode.

In the calculated structures of the PI dimer, the energies of HOMO (6.68 eV) and LUMO (4.77 eV) agree with the energy of frontier orbitals for related diimides calculated by the PBE0-D3/Def2-TZVPD method.[26]

Thus, it was demonstrated that the addition of Aerosil 380 SiO_2 nanoparticles enhanced not only the discharge capacity stability for 300 charge–discharge cycles but also the average cell voltage by 0.06 V, which led to an increase in the power characteristics of the battery. The SiO_2 nanoparticles served as a framework for PI polyimide fixed on their surface and retained its structure upon metalation with Na.

This work was supported by Ministry of Education and Science of the Russian Federation, project nos. AAAA-A19-119071190044-3 (Experiment) and AAAA-A19-119111390022-2 (Quantum-chemical modeling). The work was partially fulfilled using the equipment of the Analytical Center for Collective Use of the Scientific Center in Chernogolovka of the RAS (project no. AAAA-A19-119061890019-5).

References

1 T. Perveen, M. Siddiq, N. Shahzad, R. Ihsan, A. Ahmad and M. I. Shahzad, *Renewable Sustainable Energy Rev.*, 2020, **119**, 109549.
2 A. M. Skundin, T. L. Kulova and A. B. Yaroslavtsev, *Russ. J. Electrochem.*, 2018, **54**, 113 (*Elektrokhimiya*, 2018, **54**, 131).
3 J. J. Abraham, C. R. A. Arro, H. A. Tariq, R. Kahraman, S. Al-Qaradawi, T. M. Al Tahtamouni and R. A. Shakoor, *J. Power Sources*, 2021, **506**, 230098.
4 K. Holguin, M. Mohammadiroudbari, K. Q. Qin and C. Luo, *J. Mater. Chem. A*, 2021, **9**, 19083.
5 R. Puttaswamy, N. S. Kotrappanavar and D. Ghosh, *Mater. Adv*., 2021, **2**, 5006.
6 R. Usiskin, Y. Lu, J. Popovic, M. Law, P. Balaya, Y.-S. Hu and J. Maier, *Nat. Rev*. *Mater*., 2021, **6**, 1020.
7 H. Banda, D. Damien, K. Nagarajan, M. Hariharan and M. M. Shaijumon, *J. Mater. Chem. A*, 2015, **3**, 10453.
8 O. V. Yarmolenko, O. E. Romanyuk, A. A. Slesarenko, G. R. Baymuratova, N. I. Shuvalova, A. V. Mumyatov, P. A. Troshin and A. F. Shestakov, *Russ. J. Electrochem.*, 2019, **55**, 254 (*Elektrokhimiya*, 2019, **55**, 394).
9 A. F. Shestakov, O. E. Romanuyk, A. V. Mumyatov, S. Y. Luchkin, A. A. Slesarenko, O. V. Yarmolenko, K. J. Stevenson and P. A. Troshin, *J. Electroanal. Chem.*, 2019, **836**, 143.
10 G. R. Baymuratova, A. V. Mumyatov, R. R. Kapaev, P. A. Troshin and O. V. Yarmolenko, *Russ. J. Electrochem.*, 2021, **57**, 725 (*Elektrokhimiya*, 2021, **57**, 429).
11 Y. Huang, K. Li, J. Liu, X. Zhong, X. Duan, I. Shakir and Y. Xu, *J. Mater. Chem. A*, 2017, **5**, 2710.
12 Y. Zhang, Y. An, S. Dong, J. Jiang, H. Dou and X. Zhang, *J. Phys. Chem. C*, 2018, **122**, 22294.
13 K. J. Kalita, I. Giri and R. K. Vijayaraghavan, *RSC Adv.*, 2021, **11**, 33703.
14 Q. Cheng, W. He, X. Zhang, M. Li and X. Song, *RSC Adv.*, 2016, **6**, 10250.
15 Y. Wang, S. Wang, J. Fang, L.-X. Ding and H. A. Wang, *J. Membr. Sci.*, 2017, **537**, 248.
16 L. Liu, F. Lv, P. Li, L. Ding, W. Tong, P. K. Chu and Y. Zhang, *Composites*, *Part A*, 2016, **84**, 292.
17 S. Liu, L. Deng, W. Guo, C. Zhang, X. Liu and J. Luo, *Adv. Mater.*, 2019, **31**, 1807585.
18 F. Jiang, T. Li, P. Ju, J. Sun, C. Liu, Y. Li, X. Sun and C. Chen, *Nanoscale Adv*., 2019, **1**, 4989.
19 A. V. Yudina, M. P. Berezin, G. R. Baymuratova, N. I. Shuvalova and O. V. Yarmolenko, *Russ. Chem. Bull.*, 2017, **66**, 1278.
20 O. V. Yarmolenko, K. G. Khatmullina, G. R. Baimuratova, G. Z. Tulibaeva, L. M. Bogdanova and A. F. Shestakov, *Mendeleev Commun*., 2018, **28**, 41.
21 S. A. Baskakov, R. A. Manzhos, A. S. Lobach, Y. V. Baskakova, A. V. Kulikov, V. M. Martynenko, F. O. Milovich, Y. Kumar, A. Michtchenko, E. N. Kabachkov, A. G. Krivenko and Y. M. Shulga, *J. Non-Cryst. Solids*, 2018, **498**, 236.
22 Y. A. Golubev, N. N. Rozhkova, E. N. Kabachkov, Y. M. Shul'ga, K. Natkaniec-Hołderna, I. Natkaniec, I. V. Antonets, B. A. Makeev, N. A. Popova, V. A. Popova and E. F. Sheka, *J. Non-Cryst. Solids*, 2019, **524**, 119608.
23 P. Perdew, K. Burke and M. Ernzerhof, *Phys. Rev. Lett*., 1996, **77**, 3865.
24 W. J. Stevens, H. Basch and M. J. Krauss, *J. Chem. Phys.*, 1984, **81**, 6026.
25 D. N. Laikov, *Chem. Phys. Lett*., 1997, **281**, 151.
26 E. A. Komissarova, V. E. Zhulanov, I. G. Mokrushin, A. N. Vasyanin, E. V. Shklyaeva and G. G. Abashev, *Russ. Chem. Bull.*, 2020, **69**, 1944.

Received: 14th March 2022; Com. 22/6826